HHS Public Access

Author manuscript

Traffic. Author manuscript; available in PMC 2018 February 01.

Published in final edited form as:

Traffic. 2017 February ; 18(2): 134–144. doi:10.1111/tra.12462.

Distinct complexes of yeast Snx4 family SNX-BARs mediate retrograde trafficking of Snc1 and Atg27

Mengxiao Ma, **Christopher G. Burd**[*], and **Richard J. Chi**[1,*]

Department of Cell Biology, Yale School of Medicine, New Haven, CT

[1]Department of Biological Sciences, University of North Carolina at Charlotte

Abstract

The yeast *SNX4* sub-family of SNX-BAR proteins, Snx4/Atg24, Snx41, and Atg20/Snx42, are required for endocytic recycling and selective autophagy. Here we show that Snx4 forms two functionally distinct heterodimers: Snx4–Atg20 and Snx4–Snx41. Each heterodimer coats an endosome-derived tubule that mediates retrograde sorting of distinct cargo; the v-SNARE, Snc1, is a cargo of the Snx4-Atg20 pathway, and Snx4-Snx41 mediates retrograde sorting of Atg27, an integral membrane protein implicated in selective autophagy. Live cell imaging of individual endosomes shows that Snx4 and the Vps5-Vps17 retromer SNX-BAR heterodimer operate concurrently on a maturing endosome. Consistent with this, the yeast dynamin family protein, Vps1, which was previously shown to promote fission of retromer-coated tubules, promotes fission of Snx4-Atg20 coated tubules. The results indicate that the yeast SNX-BAR proteins coat three distinct types of endosome-derived carriers that mediate endosome-to-Golgi retrograde trafficking.

Table of contents synopsis

Live cell imaging of individual yeast endosomes shows that the Snx4 and the Vps5-Vps17 retromer sorting nexins operate concurrently on a maturing endosome. The three Snx4 family proteins form two functionally distinct heterodimers: Snx4–Atg20 and Snx4–Snx41. Each heterodimer coats an endosome-derived tubule that mediates retrograde sorting of distinct cargo; the v-SNARE, Snc1, is a cargo of the Snx4-Atg20 pathway, and Snx4-Snx41 mediates retrograde sorting of Atg27, an integral membrane protein implicated in selective autophagy.

[*]Address correspondence to: Christopher Burd, Department of Cell Biology, Yale University School of Medicine, New Haven, Connecticut 06520, Tel: 203-737-6161, christopher.burd@yale.edu. Richard Chi, Department of Biological Sciences, University of North Carolina at Charlotte, Charlotte, North Carolina 28223, Tel: 704-687-8697, rchi1@uncc.edu.

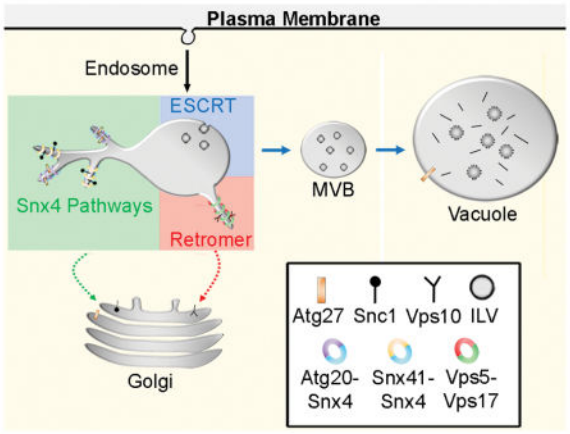

Keywords

Atg27; SNX-BAR; retromer; Vps1; endosome; autophagy

INTRODUCTION

At the endosome, sorting of molecules (termed, “cargo”) into Golgi-directed retrograde and PM-directed recycling pathways is initiated at the tubular endosomal network (TEN), a network of tubules that emanate from a vacuolar domain of the endosome.[1] One major family of proteins that is recruited to the TEN to facilitate cargo sorting is the SNX-BAR family.[2] SNX-BAR proteins constitute a sub-family of Bin-Amphiphysin-Rvs (BAR) domain containing proteins, which are characterized by their ability to scaffold high membrane curvature, such as that found in the TEN and endosomal transport carriers (ETCs).[3–6] They are distinguished by a C-terminal BAR domain and a N-terminal phox homology (PX) domain that typically recognizes PtdIns3*P*, a signaling lipid that is enriched in the endosome membrane.[7,8] Dimerization mediated by the BAR domain generates a concave membrane-binding surface that allows these proteins to sense domains of high positive membrane curvature.[6] Tip-to-tip oligomerization of SNX-BAR dimers allows them to form a membrane coat that can drive a transition in membrane topology from a molecularly flat membrane to a membrane tubule.[9] Most organisms, including *Saccharomyces cerevisiae* (yeast), which is used in this study, express multiple SNX-BAR proteins and this is thought to underlie the diversity of endosome cargo export pathways.[2]

It is currently unclear how the formation of distinct SNX-BAR coated carriers is integrated within the endosome maturation pathway. The relatively simple endo-vacuolar system of yeast provides an excellent experimental setting to address this question. The yeast genome encodes six SNX-BAR proteins with homologous counterparts in the human genome.[2] The yeast SNX4-related sub-family of SNX-BARs is composed of three members, Snx4, Snx41, and Atg20, which are proposed to function at an early (also called, ‘post-Golgi’) endosome, upstream of the Vps5 and Vps17 heterodimeric SNX-BARs that function with retromer at the late (also called, ‘pre-vacuolar’) endosome.[10,11] However, the assignment of Snx4 family proteins to an early endosome is based chiefly on genetic epistasis tests which do not

distinguish their cellular site(s) of action. In this study, we establish that Snx4, Snx41 and Atg20 localize to endosomes, most of which are also decorated by Vps5-Vps17, indicating that they act concurrently during endosome maturation.

Deletion of *SNX4*, also called *ATG24*, or *ATG20*, also called *SNX42*, results in deficient turnover of proteins in the lysosome-like vacuole via selective autophagy pathways, though the specific functions of the encoded proteins in autophagy have proven elusive to define.[12–15] An indirect role for Snx4 and Atg20 in the cargo-selective cytoplasm-to-vacuole arm of the autophagy pathway has been proposed whereby they function to maintain a Golgi-localized pool of Atg9, an integral membrane component of the autophagy machinery, by mediating endosome-to Golgi transport of Atg9.[16,17] However, this is unlikely to fully explain the role(s) of Snx4-Atg20 in autophagy because Atg9 can be trafficked from the endosome to the Golgi via redundant pathways.[16,17] Here, we describe an endosome-to-Golgi retrograde trafficking pathway that relies on a previously unrecognized Snx4-Snx41 SNX-BAR heterodimer to sort Atg27, an integral membrane protein required for autophagy,[18,19] to the Golgi apparatus.

RESULTS AND DISCUSSION

High throughput protein interaction screening and immunopurification experiments employing ectopically expressed Protein A-tagged proteins provide evidence of physical interactions between all three Snx4 family proteins.[10,12,20,21] However, most of these results were published prior to the discovery that the BAR domain is a dimeric structural module, so the full physiological significance of the observed interactions was not appreciated; moreover, it was proposed that the three proteins are components of a single complex.[10] We reasoned that intracellular targeting of individual Snx4 family proteins is dependent upon their association with its partner in the SNX-BAR dimer. Thus, to address functional interactions amongst Snx4 family proteins, we used live cell fluorescence microscopy to compare the cellular distributions of each fluorescently tagged Snx4 protein in wild-type and mutant cells containing deletions of each of the other *SNX4* family genes. Each Snx4 family protein was expressed from its native locus with a C-terminal tandem green fluorescent protein (2xGFP) and the functionality of the tagged proteins was confirmed by proper localization of mCherry-tagged Snc1, a v-SNARE molecule that is an established retrograde cargo of the Snx4 pathway.[10]

In wild-type cells, all three Snx4 proteins display a punctate distribution typical of Golgi/endosome-localized proteins, confirming previously published reports (Fig. 1A).[10,12,22] Quantitative colocalization analysis shows that Snx4 colocalizes equally with Snx41 and Atg20 (Fig. 1B; Pearson's correlations, R_{ave}=0.49 (n=31), R_{ave}=0.52 (n=31), respectively). The localization of Snx4 to an endosome requires the presence of either Snx41 or Atg20; Snx4-2xGFP maintains a punctate distribution in *snx41Δ* and *atg20Δ* cells similar to that in wild-type cells, but it localizes to the cytosol of *snx41Δ atg20Δ* cells (Fig. 1A). Similarly, Atg20 localizes to the cytosol in *snx4Δ* cells. We note that Snx4-2xGFP and Snx41-2xGFP puncta are observed in some *snx41Δ atg20Δ* and *snx4Δatg20Δ* double mutant cells, respectively (Fig. 1A). However, the motion of these puncta is less dynamic compared to the puncta observed in wild-type cells (unpublished observations). Co-immunoprecipitation

analyses designed to detect homodimers of each protein in appropriate deletion mutant cells did not provide any evidence for homodimerization of either protein under conditions where Snx4-Snx41 dimers were recovered (data not shown). For Snx4, this result confirms the conclusion of Hettema et al.[10] that Snx4 does not form a homodimer. The dependencies of Atg20 and Snx41 on Snx4 for endosome localization explain the requirement for both Snx4 and Atg20 in the CVT pathway, and suggest that Snx4 and Snx41 form a functionally distinct SNX-BAR dimer.

Snx4 family and retromer SNX-BARs coat distinct endosomal tubules

A general function of SNX-BAR proteins is to serve as coat proteins of endosome-derived, tubular transport carriers.[2] We previously reported that retromer SNX-BAR proteins (Vps5 and Vps17) and Mvp1/Snx8 co-decorate tubules containing retrograde cargo that bud and fission from an endosome,[23] and we sought to determine if Snx4 family proteins also decorate endosome-derived tubules. Accordingly, we used live cell time-lapse fluorescence microscopy of single endosomes decorated by C-terminal 2xGFP tagged Snx4, Snx41, and Atg20. Figure 2A shows example galleries in which each Snx4 family protein is observed to decorate a ‘mother’ endosome from which SNX-BAR coated tubules can be seen to bud and undergo fission. We were unable to determine if these SNX-BAR coated tubules contain Snc1, the best characterized cargo of the ‘SNX4 pathway’,[10] due to the low abundance of Snc1 in the endosomal system. Nevertheless, given the established roles of SNX-BAR proteins in coating endosome-derived transport carriers, and the exclusion of vacuole-directed cargo (i.e., Mup1, described later) from Snx4 family coated tubules, we conclude that Snx4 family proteins coat endosome-derived transport carriers.

Next, the spatial and temporal dynamics of Snx4 family proteins within the endosomal system was characterized. The results of genetic epistasis experiments have led to the proposal that the Snx4 family SNX-BARs operate at the early/post-Golgi endosome upstream of retromer, which is proposed to function at the late/pre-vacuolar endosome.[10,11] This model predicts that Snx4 proteins and retromer SNX-BARs should decorate distinct populations of endosomes and that internalized cargo *en route* to the vacuole should pass through a Snx4 decorated endosome prior to a retromer decorated endosome. To test this, we conducted fluorescence microscopy of cells co-expressing tagged forms of Snx4 and a retromer SNX-BAR, Vps17. To observe the SNX-BAR proteins within the context of a maturing endosome, we monitored Snx4 and Vps17 dynamics on an endosome containing Mup1-mTagBFP2, a fluorescently tagged methionine transporter that is targeted to the vacuole upon addition of methionine to the growth medium of methionine-starved cells.[24] Fifteen minutes after methionine addition, Mup1-mTagBFP2 containing endosomes are observed to be decorated by both Snx4 and Vps17 (Fig. 2B). Surprisingly, both Snx4 and Vps17 decorate a largely overlapping population of endosomes (Fig. 2B), as measured by colocalization analysis (R_{ave}=0.5 (n=20)). Furthermore, we observed that in cells expressing both Snx4-2xGFP and Vps17-2xRFP, tubules emanating from an endosome are decorated with either Snx4 or Vps17, but not both proteins (Fig. 2C, Supplemental Video 1); of 100 scored tubules, only three appeared to contain both Snx4 and Vps17 (Fig. 2D). These data account for the distinct cargo specificities of the Snx4 and retromer pathways; each SNX-BAR decorates a distinct transport carrier that buds from a maturing endosome. This finding

is also consistent with redundancies of these sorting machineries that have been observed for some cell surface recycling proteins, such as the Can1 arginine transporter.[11,25]

Next, we compared Snx4 and Vps17 localization to a protein of the degradative multivesicular body (MVB) pathway, Did2, and observed that it decorates Snx4- and Vps17-double positive endosomes, as well as endosomes that lack either SNX-BAR (Fig. 3A). Time lapse fluorescence microscopy revealed that Did2 remains on the endosome while the levels of Snx4 and Vps17 decrease, ultimately to undetectable levels (Fig. 3B). We note that Vps17 signal disappears from the endosome at an earlier time point than Snx4, however, this is likely due to faster photobleaching of Vps17-mTagRuby2 compared to Snx4-2xGFP. In the cases of an endosome decorated by all three proteins, each protein appears to occupy a distinct domain with a small region of overlap; this is particularly apparent in a line scan across an endosome (Fig. 3A). These results indicate that these proteins occupy distinct domains on the endosome membrane, similar to the mosaic of domains on mammalian endosomes.[26] The results indicate that, contrary to the assignment of Snx4 family and retromer SNX-BARs to distinct endosomes, these proteins act concurrently on a maturing endosome. This conclusion is further supported by a recent study showing that endocytic cargo (fluorescently labeled alpha factor) arrives at an endosome decorated with Snx41 or Vps17 with identical kinetics.[22]

The dynamin-like protein, Vps1, is required for fission of Snx4-coated endosome-derived tubules

The dynamin-related GTPase, Vps1, is required for retromer-dependent retrograde trafficking from the endosome,[23] as well as proper trafficking of Snc1, a Snx4-Atg20 retrograde cargo.[27,28] To determine if Vps1 also plays a role in Snx4-mediated trafficking, we first quantified the numbers of endosomes in wild-type versus *vps1*Δ cells expressing Snx4-2xGFP and Vps17-2xRFP as a control. As expected from our published observations of Vps17 in *vps1Δ* cells,[23] and the co-localization of Snx4 and Vps17 (Fig. 2, 4A), there is an increase in the number of both Vps17-decorated and Snx4-decorated endosomes in *vps1*Δ cells (Fig. 4A; [23]). This is also consistent with the enlarged Vps17-decorated endosomes we have seen in *vps1*Δ cells previously.[23] Time-lapse fluorescence microscopy (Fig. 4B) revealed a clear delay in the fission of Snx4-2xGFP coated tubules in *vps1*Δ cells, inferred from measurements of coated tubule lifetime.[23] This was observed for both Snx4 tubules and, as previously noted, for Vps17 tubules (Fig 5B, C).[23] From these results, we conclude that Vps1 plays a general role in promoting fission of SNX-BAR coated tubules from the endosome.

Snc1 is sorted to the vacuole of snx4Δ and atg20Δ mutant cells

The best characterized cargo of Snx4 family trafficking pathways is Snc1, a v-SNARE of secretory vesicles that is retrieved back to the Golgi by endocytosis and subsequent retrograde trafficking. A prior study[10] reported that Snc1 localizes to the vacuole of *snx4Δ* and *atg20Δ* mutant cells, indicating that Snx4 and Atg20 are required for recycling of GFP-Snc1, and we confirmed these results; 95% of *snx4Δ* cells and 72% of *atg20Δ* cells have vacuole localization of GFP-Snc1. In addition, Hettema et al.[10] reported that GFP-Snc1 was partially mislocalized in *snx41Δ* cells, however, we observed that GFP-Snc1 localization in

wild-type and *snx41Δ* cells is indistinguishable, as less than 10% of cells of each strain have mislocalized GFP-Snc1 (Fig. 5). These results were confirmed by an anti-GFP immunoblot showing the processing of full-length GFP-Snc1 to free GFP (by vacuolar proteases) in *snx4Δ* and *atg20Δ* cells, but not in *snx41Δ* cells (Fig. 5B). In view of the dependence of Atg20 on Snx4 for its endosome membrane targeting (Fig. 1A), the results suggest that Snc1 recycling is mediated by a Snx4-Atg20 SNX-BAR heterodimer.

Retrograde sorting of Atg27 requires Snx4 and Snx41

There are two integral membrane protein components of the yeast autophagy pathway, Atg9 and Atg27, and GFP-tagged forms of each protein are broadly distributed to organelles of the endo-vacuolar system (Golgi, endosome, vacuole) and the autophagy pathway (PAS, autophagosome).[17–19,29,30] One proposed role for Snx4-Atg20 in autophagy is retrograde trafficking of Atg9 from the endosome to the Golgi, in order to maintain a reservoir of Atg9 at the Golgi, the proposed source of ‘Atg9 vesicles’ that function early in autophagosome biogenesis.[16,17,29] We therefore compared localization of GFP tagged Atg27 in Snx4 family deletion mutants, as loss of retrograde sorting will result in delivery to the vacuole. Because there is a substantial pool of Atg27-GFP in the vacuole membrane in wild-type cells,[18] it was difficult to gauge the amounts of Atg27-GFP on the vacuole membrane in wild-type versus mutant cells. Since vacuole localization of Atg27-GFP requires a functional AP3-dependent sorting signal, we examined a form of Atg27, first described by Segarra et al.,[18] in which the AP3 sorting signal has been deleted (termed, “Atg27-ΔYSAV-2xGFP”) (Fig. 6A). In agreement with Segarra et al.,[18] less than 15% of wild-type cells displayed Atg27-ΔYSAV-2xGFP circumferential vacuole membrane localization, and this is also true for *atg20Δ* cells. In striking contrast, Atg27-ΔYSAV-2xGFP localized to the vacuole membrane in more than 60% of *snx4Δ* and *snx41Δ* cells (Fig. 6E). These data indicate that Snx4 and Snx41, likely as a Snx4-Snx41 heterodimer, are required for endosome-to-Golgi trafficking of Atg27. In consideration of the Snc1 and Atg27 trafficking data, we conclude that Snx4 is a common subunit of two functional distinct SNX-BAR dimers, Snx4-Atg20 and Snx4-Snx41. Cargo specificity must be conferred by the unique subunits of the dimers; Atg20 confers specificity for Snc1 trafficking, and Snx41 confers specificity for trafficking of Atg27.

Curiously, a version of the Atg27-GFP fusion protein with a functional AP3 sorting signal,[18] which we term “Atg27-link-2xGFP”, does not appear to be mislocalized in *snx4Δ* and *snx41Δ* cells (Fig. 7). This apparent conflict with the distribution of Atg27-ΔYSAV-2xGFP in these cells is readily explained by the masking of the effect of deleting *SNX4* or *SNX41* by AP3-dependent Golgi-to-vacuole trafficking of Atg27-link-2xGFP. The results of an additional experiment, in which we tested if autophagy induction influences the distribution of Atg27, further supports this view (Fig. 7). In wild-type and *atg20*Δ cells incubated for four hours in medium containing rapamycin (0.2μg/mL), Atg27-link-2xGFP no longer localizes to the vacuole (Fig. 7A, S1). However, it appears to remain associated with the vacuole membrane in rapamycin-treated *snx4Δ* cells and *snx41Δ* cells (Fig. 7B, C). These results suggest that rapamycin induces mobilization of Atg27 from the vacuole membrane, and this is corroborated by subcellular fractionation experiments (Fig. S2). We note that the extended period of time (>4 hours) required for Atg27-link-2xGFP to be depleted from the

vacuole membrane explains why Segarra et al.[18] did not observe this effect of rapamycin after just 2 hours incubation. No reduction in the amounts of Atg27-link-2xGFP, or cleavage of the GFP moiety from the full length fusion protein, is observed by anti-GFP immunoblotting of lysates of wild-type or *snx4Δ* cells incubated with or without rapamycin (Fig. S2), indicating that Atg27-link-2xGFP is not delivered to the vacuole lumen and degraded during rapamycin treatment. We have never observed Snx4 or Snx41 to decorate the vacuole membrane under any circumstances in wild-type cells, so it is unlikely that Snx4-Snx41 mediates export from the vacuole. Rather, these observations are readily explained by the role of Snx4-Snx41 in retrograde sorting of Atg27; when retrograde sorting fails, as it does in *snx4Δ* cells and *snx41Δ* cells, Atg27 is delivered to the vacuole membrane via the endosome maturation pathway (Fig. 8). Loss of AP3-dependent trafficking of Atg27 does not impact autophagy,[18] and *snx41Δ* mutants are not reported to have defects in autophagy, so the physiological role the Snx4-Snx41 pathway in unclear. In addition, the role of the vacuolar pool of Atg27 and the mechanism by which it is removed from the vacuole membrane, remain open questions. It is of fundamental interest to determine how Atg27 is mobilized from the vacuole membrane, as this may constitute a general mechanism used to modulate the composition of the vacuole membrane.[31]

Retrograde sorting by yeast SNX-BARs

When considered with the body of relevant literature, the results presented here indicate that four distinct SNX-BAR dimers, Snx4-Atg20, Snx4-Snx41, Mvp1-Mvp1, and Vps5-Vps17, export cargo from a maturing endosome (Fig. 8). Although not formally demonstrated for Snx4-Atg20 and Snx4-Snx41, each SNX-BAR pair likely coats a distinct ETC, with the exception of Mvp1, which is incorporated with Vps5-Vps17 into some ETCs.[23] As different cargo proteins are uniquely affected by the loss of individual SNX-BARs, we suggest that three distinct SNX-BAR-mediated cargo export pathways operate on the yeast endosome (Fig. 8). Surprisingly, we find that Snx4 family and retromer SNX-BARs decorate a largely (though not completely) overlapping population of endosomes, which contrasts with models positing that Snx4 family and retromer SNX-BARs operate on distinct populations of endosomes.[10,11] Each SNX-BAR protein operates independently of the other SNX-BARs, rather than via a sequential mechanism. What is the advantage of multiple retrograde pathways that sort molecules to the same destination - the Golgi apparatus? For the cases of Snx4-Atg20 and Snx4-Snx41, cargo specificity is conferred by the unique subunit, so multiple SNX-BARs expands the repertoire of cargo that can be exported from the endosome. In addition, different SNX-BAR-coated ETCs might mediate trafficking to distinct entry sites within the TGN, which would prevent mixing of the different cargo populations. It is also intriguing that trafficking of the two integral membrane protein components of the autophagy pathway, Atg9 and Atg27, to the PAS is inter-dependent,[18,19,30] yet each protein is sorted from the endosome to the Golgi via a distinct pathway, with Atg9 relying on the Snx4-Atg20 pathway[16,17] and Atg27 relying on Snx4-Snx41 pathway. This arrangement allows for segregation of Atg9 and Atg27 and for the amounts of each protein in the Golgi to be controlled independently. The mechanism(s) of cargo selection for the Snx4-Atg20 and Snx4-Snx41 pathways is largely unknown and this is an important question to be addressed in the future. In the case of the retromer pathway, the Vps26-Vps29-Vps35 retromer trimer mediates cargo selection, suggesting that Vps5-Vps17

does not impart cargo specificity. A cargo of the Snx4-Atg20 retrograde pathway, Snc1, can be chemically crosslinked to Snx4,[10] though it is not clear if Snx4-Atg20 directly recognizes Snc1. The identification of a Snx4-Snx41 retrograde pathway and a cargo of this pathway (Atg27) will facilitate future studies into the basis of cargo selection within the Snx4-mediated pathways.

MATERIALS AND METHODS

Yeast strains and culture conditions

Yeast strains were constructed in BY4742 (*MATα his3-1*, *leu2-0*, *met15-0*, and *ura3-0)* by homologous recombination of gene-targeted, polymerase chain reaction (PCR)-generated DNAs using the method of Longtine et al.[32] Mutant strains used were either derived from the EUROSCARF *KANMX* deletion collection (Open Biosystems/Thermo Scientific, Waltham, MA) or produced by replacement of the complete reading frame with the *HIS3MX6* or *URA3* cassette. Gene deletions were confirmed by PCR amplification of the deleted locus. Atg27-ΔYSAV-2xGFP yeast strains were constructed using a forward primer just upstream of YSAV, resulting in a deletion of YSAV and tagging with link-2xGFP. Atg27-link-2xGFP yeast strains were constructed using a forward primer that introduced a 17 amino acid linker between Atg27 and 2xGFP.

Cells were grown in standard synthetic complete medium lacking nutrients required to maintain selection for auxotrophic markers and/or plasmids.[33] For experiments using Mup1-mTagBFP2, cells were grown overnight at 24°C to early log phase in synthetic complete medium lacking methionine. Cultures were supplemented to 20 μg/ml methionine to induce endocytosis of Mup1 and images were captured within 15 minutes of addition.

For rapamycin treatment and FM4-64 labeling, 0.2 μg/mL of rapamycin (R-5000, LC laboratories) was added to early log phase cell cultures in standard synthetic complete medium and incubated at 30°C, then concentrated and incubated with 32nM FM4-64 for 20 min in YPD, washed and resuspended in fresh synthetic complete medium containing 0.2 μg/mL of rapamycin for a total of 4 hr rapamycin incubation time.

Subcellular fractionation and immunoblotting

For subcellular fractionation studies, spheroplasts were made from wild-type or *snx4Δ* cells expressing Atg27-link-2xGFP and processed as described.[34] Briefly, cells were grown under standard vegetative or autophagy inducing conditions to OD600 ≈ 0.5, as described above. Spheroplasts from 30×10^7 cells were harvested per yeast strain and lysed. Crude lysate was clarified by centrifugation at 1000 g for 5 min at 4°C, generating P3 and S3 fractions. The supernatant (S3) was centrifuged at 13,000 g for 10 min at 4°C, generating P13 and S13 fractions. The S13 fraction was then centrifuged at 100,000 g for 1hr at 4°C using Optima Max-XP benchtop ultracentrifuge (Beckman Coulter), generating P100 and S100 fractions. All fractions were precipitated by trichloroacetic acid to 10% final concentration. Fractions were resolved by 10% polyacrylamide gels, transferred onto standard 0.45 μm nitrocellulose and immunoblotted.

For semi-quantitative western blot analysis of GFP-fusion proteins, anti-GFP primary mouse monoclonal antibody (1814460, Roche) was diluted 1:2500 and Santa Cruz (sc-2055) goat anti-mouse HRP-conjugated antibody was used at 1:5000. Anti-Pgk1 at 1:5000 (Life Technologies) was used as loading controls. All enhanced chemiluminescence (ECL) blots were developed on a Chemidoc-XRS+ (Bio-Rad) and band intensities were quantified using Quanity One 1D analysis software (Bio-rad).

Light Microscopy and Image Analysis

Yeast cells from cultures grown to $OD_{600} \approx 0.5$ were mounted in growth medium, and 3D image stacks were collected at 0.3-μm z increments on a DeltaVision workstation (Applied Precision) based on an inverted microscope (IX-70; Olympus) using a 100×1.4NA oil immersion lens. Images were captured at 24°C with a front illuminated sCMOS, 2560 × 2160 pixels camera and deconvolved using the iterative-constrained algorithm and the measured point spread function. Image analysis and preparation was done using Softworx 6.1 (Applied Precision Instruments) and ImageJ v1.50d (Rasband).

For time-lapse movies, endosomes were focused in a single focal plane in cells expressing endogenously expressed C-terminal 2xGFP, 2xRFP, mTagBFP2 or mTagRuby2 fusions. For single color movies, exposure times of 100 msec resulted in an acquisition time of ~ 200 msec per interval which allowed us monitor an endosome for up to 20 seconds before photobleaching of the GFP signal. For dual color movies we routinely used exposure times of 100 msec for 2xGFP and 150 msec for 2xRFP paired with DeltaVision's Live Cell GFP/mCherry filter set which resulted in an acquisition time of ~400 msec per interval. For three color movies, a 100–150 msec exposure with 405 nm light was included to excite mTagBFP2 and was paired with DeltaVision's Standard DAPI/FITC/TRITC filter set. This allowed us to image endosome maturation and tubule budding at an acquisition time of 700–1000 msec. Movies were then 2D deconvolved using DeltaVision SoftWoRx 6.1 software and frames were compared side-by-side in a tile-view. Only linear adjustments were made to enhance overall contrast of the tubules and figures were assembled using Adobe Photoshop.

"Endosome tubule lifetime" is defined as the time point where a vesicle/tubule emerges from a mother endosome to the time point of either an apparent fission event or the movie frame where the structure completely disappears.[23] Measurements were obtained from single or dual or triple color time-lapse movies of indicated GFP, RFP, BFP fusions. Average tubule lifetimes ± s.d. were determined from 30 tubules for each condition. The Student's *t*-test was used to calculate *P*-values. Endosome tubule compositions were quantified as previously described (n=100).[23]

To visualize vacuole membrane, yeast cell cultures were incubated with FM4-64 lipophilic dye at 32nM at 30°C for 20 min in YPD, washed, and resuspended in fresh medium and grown for 120 minutes to allow FM4-64 to transit to the vacuole membrane.[35] We identify Atg27-ΔYSAV-2xGFP and Atg27-2xGFP vacuole membrane localization as non-punctate, continuous and circumferential overlapping signal with the vacuole membrane dye, FM4-64, as described in Segarra et al.[18]

Supplementary Material

Refer to Web version on PubMed Central for supplementary material.

Acknowledgments

We are grateful to Christian Ungermann and Henning Arlt for discussions, and Scott Emr for sharing unpublished data. Research reported in this publication was supported by the National Institute of General Medical Sciences of the National Institutes of Health under award number GM060221 and in part by the National Institute of General Medical Sciences of the National Institutes of Health under award number T32GM007223. R.C. was supported in part by the UNC-Charlotte Faculty Research Grants Program.

ABBREVIATIONS LIST

BAR	Bin-Amphiphysin-Rvs161 (BAR) homology
ESCRT	endosomal sorting complexes required for transport
PGK	3-phosphoglycerate kinase 1
PX	Phox homology
SNX-BAR	sorting nexin containing a BAR domain
PAS	preautophagosomsal structure
WT	wild-type

References

1. Maxfield FR, McGraw TE. Endocytic recycling. Nature reviews Molecular cell biology. 2004; 5(2): 121–132. [PubMed: 15040445]
2. Chi RJ, Harrison MS, Burd CG. Biogenesis of endosome-derived transport carriers. Cellular and molecular life sciences : CMLS. 2015; 72(18):3441–3455. [PubMed: 26022064]
3. van Weering JR, Cullen PJ. Membrane-associated cargo recycling by tubule-based endosomal sorting. Seminars in cell & developmental biology. 2014; 31:40–47. [PubMed: 24641888]
4. Peter BJ, Kent HM, Mills IG, et al. BAR domains as sensors of membrane curvature: the amphiphysin BAR structure. Science. 2004; 303(5657):495–499. [PubMed: 14645856]
5. McMahon HT, Gallop JL. Membrane curvature and mechanisms of dynamic cell membrane remodelling. Nature. 2005; 438(7068):590–596. [PubMed: 16319878]
6. Suetsugu S, Toyooka K, Senju Y. Subcellular membrane curvature mediated by the BAR domain superfamily proteins. Seminars in cell & developmental biology. 2010; 21(4):340–349. [PubMed: 19963073]
7. van Weering JR, Verkade P, Cullen PJ. SNX-BAR proteins in phosphoinositide-mediated, tubular-based endosomal sorting. Seminars in cell & developmental biology. 2010; 21(4):371–380. [PubMed: 19914387]
8. Carlton J, Bujny M, Peter BJ, et al. Sorting nexin-1 mediates tubular endosome-to-TGN transport through coincidence sensing of high-curvature membranes and 3-phosphoinositides. Current biology : CB. 2004; 14(20):1791–1800. [PubMed: 15498486]
9. van Weering JR, Sessions RB, Traer CJ, et al. Molecular basis for SNX-BAR-mediated assembly of distinct endosomal sorting tubules. The EMBO journal. 2012; 31(23):4466–4480. [PubMed: 23085988]
10. Hettema EH, Lewis MJ, Black MW, Pelham HRB. Retromer and the sorting nexins Snx4/41/42 mediate distinct retrieval pathways from yeast endosomes. The EMBO journal. 2003; 22(3):548–557. [PubMed: 12554655]

11. Shi Y, Stefan CJ, Rue SM, Teis D, Emr SD. Two novel WD40 domain-containing proteins, Ere1 and Ere2, function in the retromer-mediated endosomal recycling pathway. Molecular biology of the cell. 2011; 22(21):4093–4107. [PubMed: 21880895]
12. Nice DC, Sato TK, Stromhaug PE, Emr SD, Klionsky DJ. Cooperative binding of the cytoplasm to vacuole targeting pathway proteins, Cvt13 and Cvt20, to phosphatidylinositol 3-phosphate at the pre-autophagosomal structure is required for selective autophagy. The Journal of biological chemistry. 2002; 277(33):30198–30207. [PubMed: 12048214]
13. Okamoto K, Kondo-Okamoto N, Ohsumi Y. Mitochondria-anchored receptor Atg32 mediates degradation of mitochondria via selective autophagy. Developmental cell. 2009; 17(1):87–97. [PubMed: 19619494]
14. Kanki T, Wang K, Baba M, et al. A genomic screen for yeast mutants defective in selective mitochondria autophagy. Molecular biology of the cell. 2009; 20(22):4730–4738. [PubMed: 19793921]
15. Shpilka T, Welter E, Borovsky N, et al. Fatty acid synthase is preferentially degraded by autophagy upon nitrogen starvation in yeast. Proceedings of the National Academy of Sciences of the United States of America. 2015; 112(5):1434–1439. [PubMed: 25605918]
16. Shirahama-Noda K, Kira S, Yoshimori T, Noda T. TRAPPIII is responsible for vesicular transport from early endosomes to Golgi, facilitating Atg9 cycling in autophagy. Journal of cell science. 2013; 126(Pt 21):4963–4973. [PubMed: 23986483]
17. Ohashi Y, Munro S. Membrane delivery to the yeast autophagosome from the Golgi-endosomal system. Molecular biology of the cell. 2010; 21(22):3998–4008. [PubMed: 20861302]
18. Segarra VA, Boettner DR, Lemmon SK. Atg27 Tyrosine Sorting Motif is Important for Its Trafficking and Atg9 Localization. Traffic. 2015; 16(4):365–378. [PubMed: 25557545]
19. Yen WL, Legakis JE, Nair U, Klionsky DJ. Atg27 is required for autophagy-dependent cycling of Atg9. Molecular biology of the cell. 2007; 18(2):581–593. [PubMed: 17135291]
20. Costanzo M, Baryshnikova A, Bellay J, et al. The Genetic Landscape of a Cell. Science. 2010; 327(5964):425–431. [PubMed: 20093466]
21. Ito T, Chiba T, Ozawa R, Yoshida M, Hattori M, Sakaki Y. A comprehensive two-hybrid analysis to explore the yeast protein interactome. Proceedings of the National Academy of Sciences of the United States of America. 2001; 98(8):4569–4574. [PubMed: 11283351]
22. Arlt H, Auffarth K, Kurre R, Lisse D, Piehler J, Ungermann C. Spatiotemporal dynamics of membrane remodeling and fusion proteins during endocytic transport. Molecular biology of the cell. 2015; 26(7):1357–1370. [PubMed: 25657322]
23. Chi RJ, Liu J, West M, Wang J, Odorizzi G, Burd CG. Fission of SNX-BAR-coated endosomal retrograde transport carriers is promoted by the dynamin-related protein Vps1. The Journal of cell biology. 2014; 204(5):793–806. [PubMed: 24567361]
24. Menant A, Barbey R, Thomas D. Substrate-mediated remodeling of methionine transport by multiple ubiquitin-dependent mechanisms in yeast cells. The EMBO journal. 2006; 25(19):4436–4447. [PubMed: 16977312]
25. Quenneville NR, Chao TY, McCaffery JM, Conibear E. Domains within the GARP subunit Vps54 confer separate functions in complex assembly and early endosome recognition. Molecular biology of the cell. 2006; 17(4):1859–1870. [PubMed: 16452629]
26. Zerial M, McBride H. Rab proteins as membrane organizers. Nature reviews Molecular cell biology. 2001; 2(2):107–117. [PubMed: 11252952]
27. Smaczynska-de Rooij II, Allwood EG, Aghamohammadzadeh S, Hettema EH, Goldberg MW, Ayscough KR. A role for the dynamin-like protein Vps1 during endocytosis in yeast. Journal of cell science. 2010; 123(20):3496–3506. [PubMed: 20841380]
28. Palmer SE, Smaczynska-de R II, Marklew CJ, et al. A dynamin-actin interaction is required for vesicle scission during endocytosis in yeast. Current biology : CB. 2015; 25(7):868–878. [PubMed: 25772449]
29. Yamamoto H, Kakuta S, Watanabe TM, et al. Atg9 vesicles are an important membrane source during early steps of autophagosome formation. The Journal of cell biology. 2012; 198(2):219–233. [PubMed: 22826123]

30. Legakis JE, Yen WL, Klionsky DJ. A cycling protein complex required for selective autophagy. Autophagy. 2007; 3(5):422–432. [PubMed: 17426440]

31. Li M, Rong Y, Chuang YS, Peng D, Emr SD. Ubiquitin-dependent lysosomal membrane protein sorting and degradation. Molecular cell. 2015; 57(3):467–478. [PubMed: 25620559]

32. Longtine MS, McKenzie A 3rd, Demarini DJ, et al. Additional modules for versatile and economical PCR-based gene deletion and modification in Saccharomyces cerevisiae. Yeast. 1998; 14(10):953–961. [PubMed: 9717241]

33. Sherman, F., Fink, GR., Lawrence, LW. Methods in yeast genetics: a laboratory manual. Cold Spring Harbor, NY: Cold Spring Harbor Laboratory Press; 1979.

34. Gaynor EC, te Heesen S, Graham TR, Aebi M, Emr SD. Signal-mediated retrieval of a membrane protein from the Golgi to the ER in yeast. The Journal of cell biology. 1994; 127(3):653–665. [PubMed: 7962050]

35. Vida TA, Emr SD. A new vital stain for visualizing vacuolar membrane dynamics and endocytosis in yeast. The Journal of cell biology. 1995; 128(5):779–792. [PubMed: 7533169]

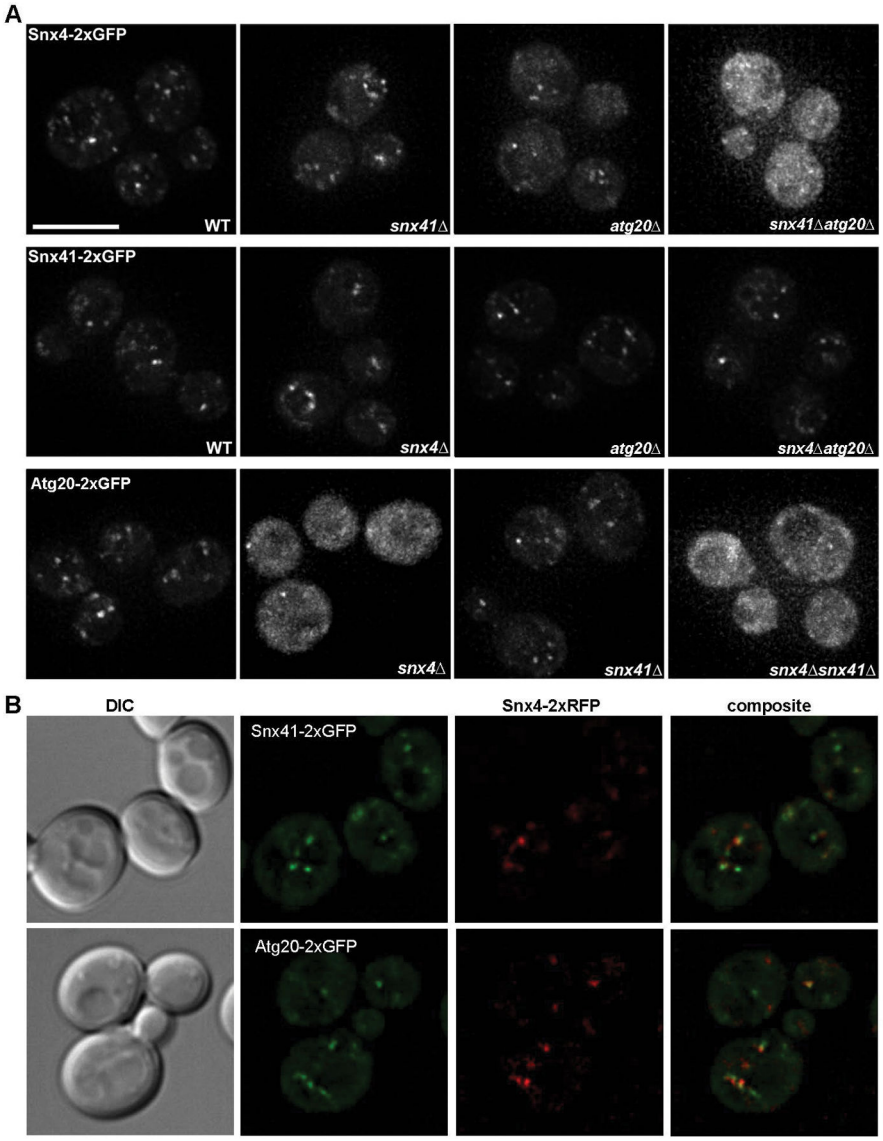

Figure 1. Snx4 is required for organelle targeting of Snx41 and Atg20

(A) Micrographs showing cells expressing Snx4, Snx41 and Atg20 as C-terminal tandem GFP fusion proteins in wild-type and the indicated mutant cells are shown. (B) Micrographs showing Snx4-2xRFP colocalization with Snx41-2xGFP and Atg20-2xGFP, Pearson's correlations are R_{ave}=0.49 (n=31), R_{ave}=0.52 (n=31), respectively. Maximum projections are shown. The scale bar indicates 5 μm.

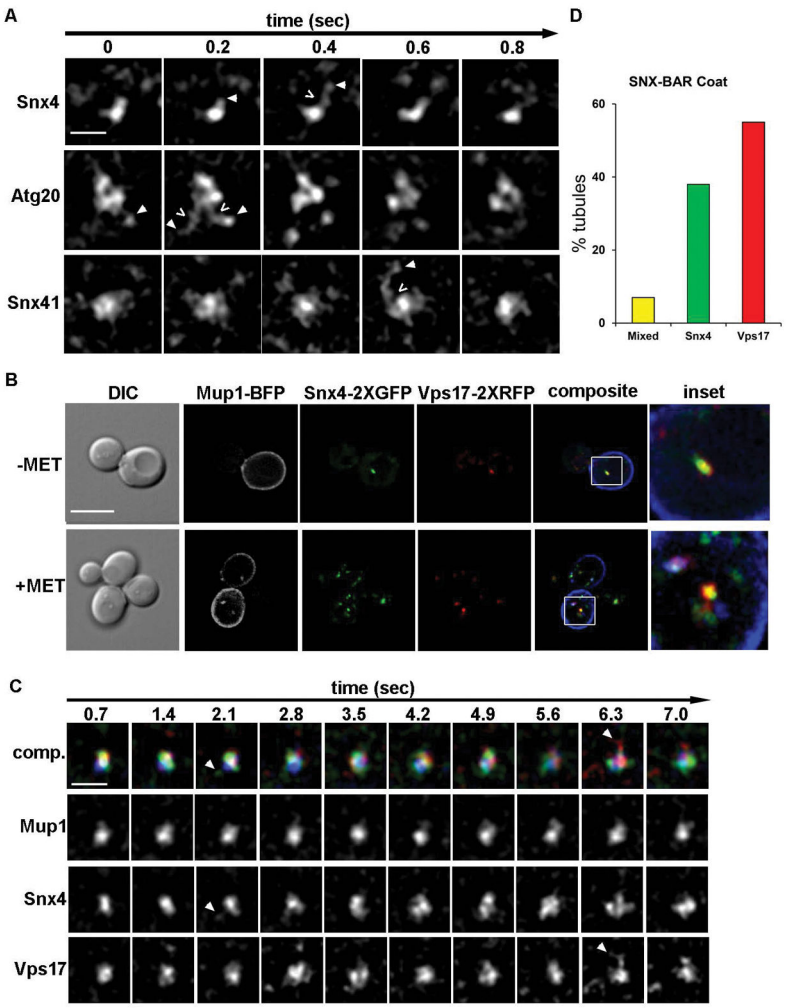

Figure 2. Snx4 family proteins coat endosome-derived membrane tubules

(A) Micrographs of Snx4-2xGFP, Atg20-2xGFP and Snx41-2xGFP decorated endosomes captured by time-lapse fluorescence deconvolution microscopy. Galleries are representative of SNX-BAR coated endosomes with an associated tubular endosomal network. Arrowheads point to tubules of interest and open arrows (<) indicate apparent fission events. Images were captured at a single focal plane and acquired at 200 msec intervals. (B) Micrographs showing cells expressing Mup1-mTagBFP2, Snx4-2xGFP, Vps17-2xRFP in methionine depleted media. Within 15 minutes of the addition of 20 μg/ml methionine, a subset of Snx4 and Vps17 (a retromer subunit) endosomes accumulated Mup1. Pearson's correlations of Snx4 and Vps17 is R_{ave}=0.5 (n=20) (C) Micrographs showing distinct tubules emanating from Mup1-mTagBFP2, Snx4-2xGFP, Vps17-2xRFP endosomes. Endosomes were captured by three-color time-lapse fluorescence deconvolution microscopy. An example of a tubule decorated by only Snx4 is shown at 2.1 sec, a tubule decorated by only Vps17-2xRFP is shown at 6.3 secs. For visual contrast, individual colors are shown in gray scale. (D) Quantitation of the different types of SNX-BAR-coated tubules. Of 100 tubules analyzed, 40% were decorated with only Snx4, 57% were decorated with only Vps17, and 3% were decorated with both.

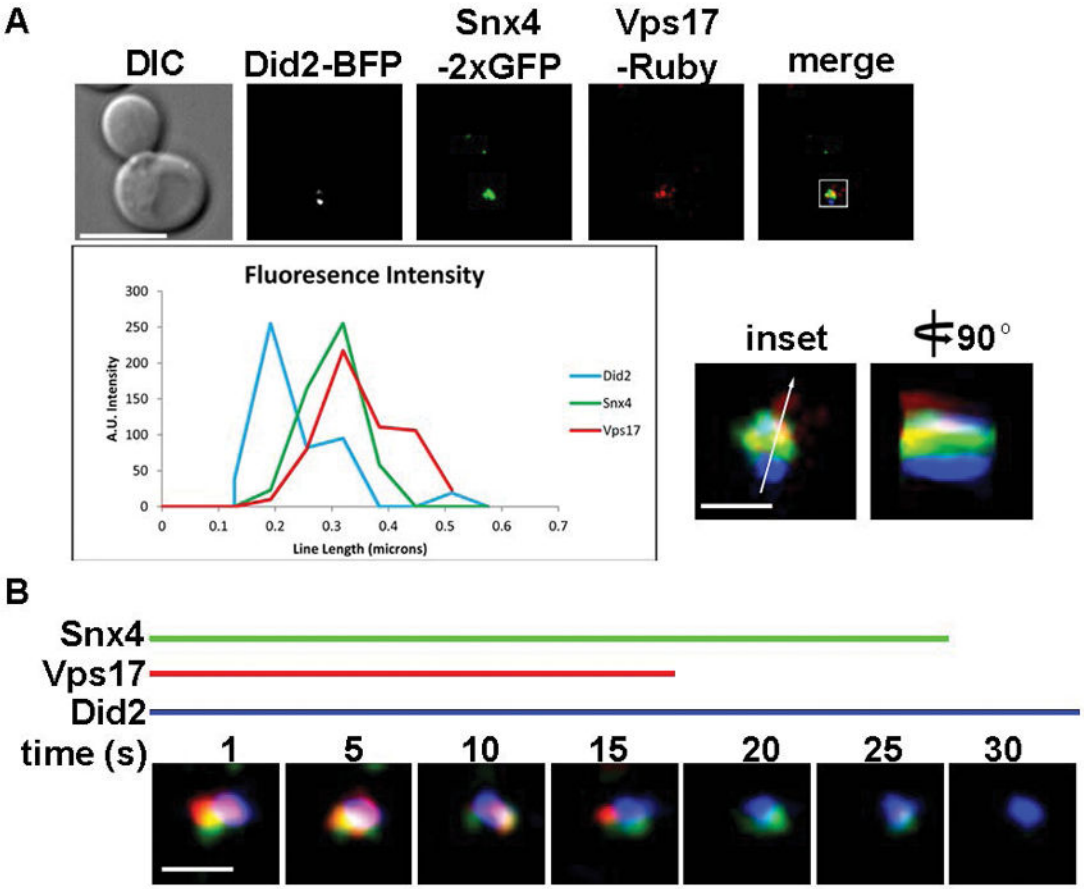

Figure 3. SNX-BARs and an ESCRT pathway component define distinct domains of the endosome membrane

(A) Micrographs showing Did2-mTagBFP2, an ESCRT pathway component, decorating a distinct domain of a common double labeled Vps17-mTagRuby2, Snx4-2xGFP endosome. The graph shows an example line scan of a typical endosome (inset). (B) Micrographs showing three-color time lapse fluorescence microscopy of an endosome. Did2 remains on the endosome while the levels of Snx4 and Vps17 gradually decrease; color-coded lines depict presence of indicated proteins in each frame. The scale bars in insets indicate 1 μm; the scale bar in whole cell micrographs indicates 5 μm.

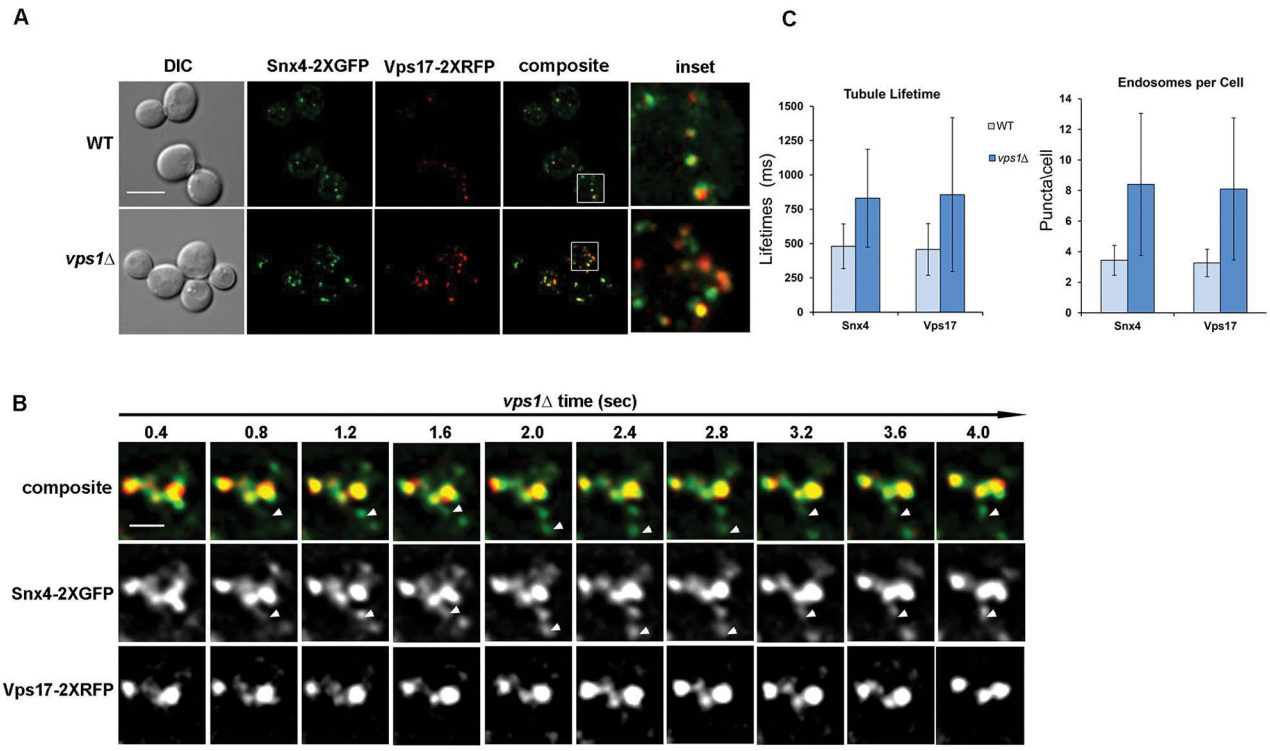

Figure 4. Vps1 dynamin-related GTPase is required for fission of Snx4 coated endosomal transport carriers

(A) Micrographs of cells expressing Snx4-2xGFP and Vp17-2xRFP were visualized in wild-type and *vps1*Δ cells. Maximum projections of deconvolved Z stacks are shown. The scale bar indicates 5 μm. (B) A time lapse gallery of Snx4-2xGFP and Vps17-2xRFP coated endosomes in *vps1*Δ cells by time-lapse fluorescence deconvolution microscopy is shown. Arrows highlight a tubule of interest in each time-lapse series. In *vps1Δ* cells, Snx4 endosomal tubules are elongated and undergo fission less frequently. (C) Left Graph, Tubule lifetimes were calculated for Snx4-2xGFP or Vps17-2xRFP coated tubules. Snx4 ($p<0.0001$) and Vps17 ($p=0.0005$) tubule lifetimes were increased in *vps1*Δ cells; Right Graph, Endosome density (puncta/cell) was calculated by using optical Z-sections (0.30 um) for Snx4-2XGFP and Vps17-2xRFPs in wildtype and *vps1*Δ cells. Both Snx4 ($p<0.0001$) and Vps17 ($p<0.0001$) endosomes are increased in *vps1*Δ cells. Standard deviations are indicated and p values were calculated using paired Student's t-test.

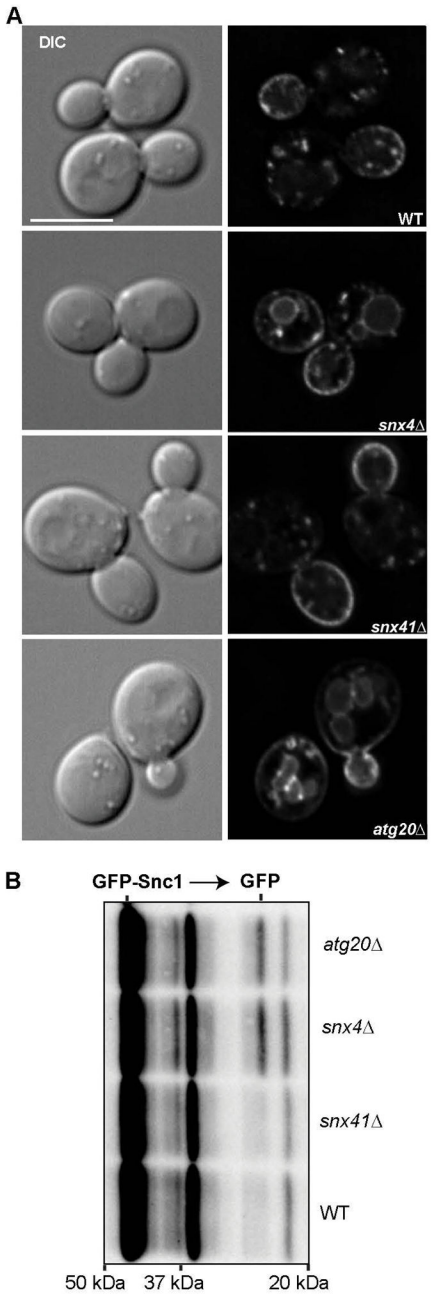

Figure 5. Snx4 and Atg20, but not Snx41, are required for plasma membrane recycling of Snc1

(A) Micrographs of ectopically expressed GFP-Snc1 in wild-type and mutant cells are shown. A single Z section from the approximate middle of each cell is shown for both fluorescent and DIC channels. (B) Cell lysates from indicated stains were probed with anti-GFP and the amount of free GFP was determined by quantitative western blot analysis. The positions of molecular mass (kDa) markers are indicated.

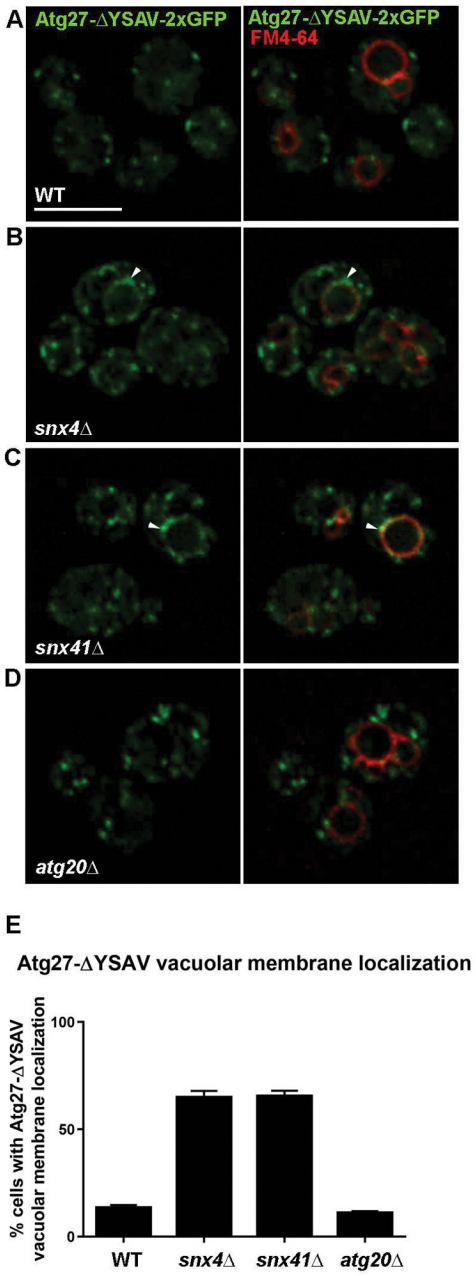

Figure 6. Snx4 and Snx41 are required to prevent accumulation of Atg27-ΔYSAV-2xGFP on the vacuole membrane

(A) Micrographs of cells expressing Atg27-ΔYSAV-2xGFP in wild-type, *snx4*Δ (B), *snx41*Δ (C), and *atg20*Δ (D) cells. Cells were grown to early log phase incubated with FM4-64 as described and imaged. Approximate middle slices of deconvolved Z stacks are shown. Vacuoles are identified with arrows. The scale bar indicates 5 μm. (E) Quantification of percent of cells with vacuolar membrane localization of Atg27-ΔYSAV-2xGFP as measured by continuous colocalization of Atg27-ΔYSAV-2xGFP with FM4-64. Error bars indicate SEM of three independent experiments.

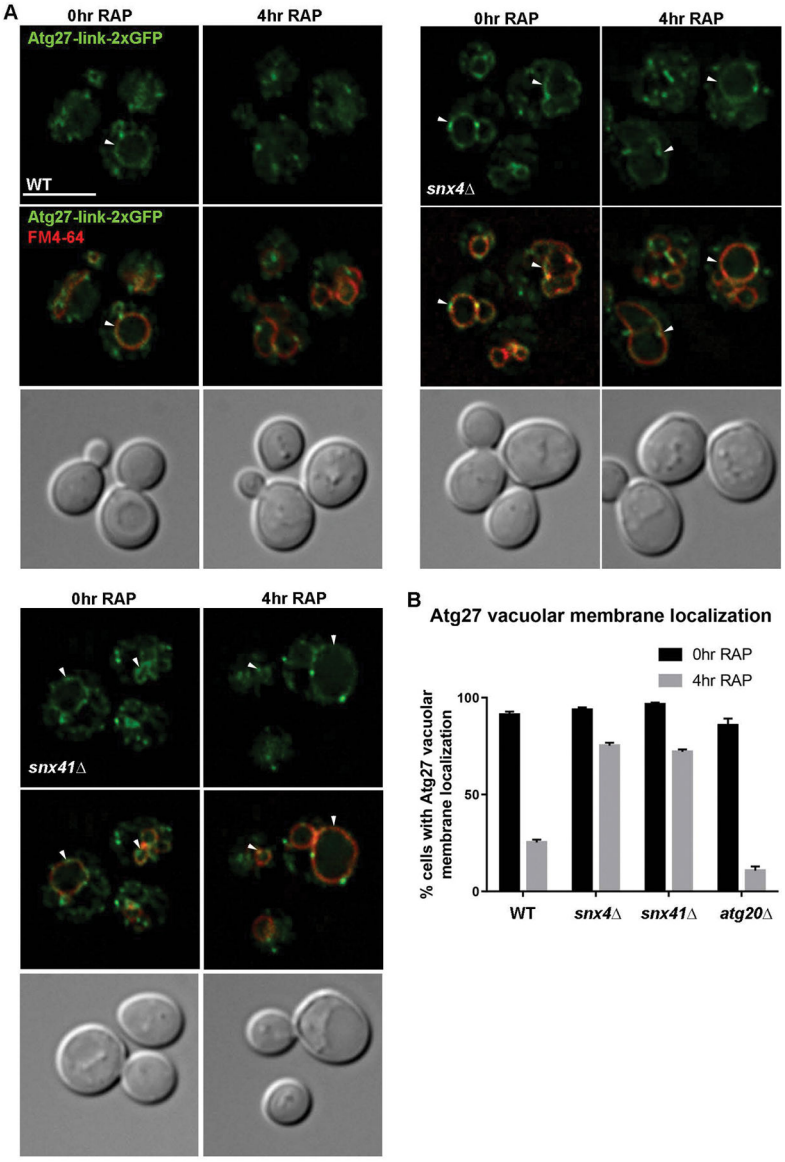

Figure 7. Atg27 fails to mobilize from the vacuole membrane in response to rapamycin treatment in *snx4*Δ and *snx41*Δ cells

(A) Micrographs of cells expressing Atg27-link-2xGFP in wild-type, *snx4*Δ (B), and *snx41*Δ (C) cells. Cells were grown to early log phase and incubated with rapamycin (0.2μg/mL) for 4 hr to induce autophagy and labeled with FM4-64 dye as described. Approximate middle slices of deconvolved Z stacks are shown. Vacuoles are identified with arrows. The scale bar indicates 5 μm. (D) Quantification of percent of cells with vacuolar membrane localization of Atg27-link-2xGFP as measured by continuous colocalization of Atg27-link-2xGFP with FM4-64. Error bars indicate SEM of three independent experiments.

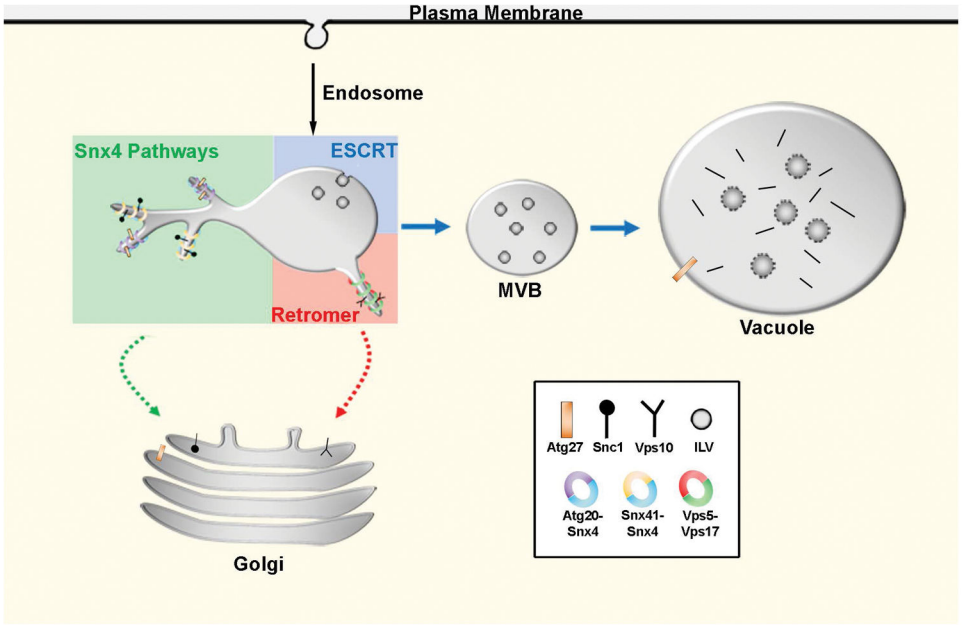

Figure 8. Summary of SNX-BAR sorting pathways in the yeast endosomal system

The endosomal maturation pathway is depicted. We propose that the Snx4 family proteins function concurrently with retromer SNX-BARs on an endosome to sort distinct cargo proteins. Snx4 dimerizes with Snx41 or Atg20, each of which confer distinct cargo specificities. Snx4-Atg20 functions on the Snc1 v-SNARE recycling pathway to transport Snc1 to the Golgi, and Snx4-Snx41 functions to transport Atg27 to the Golgi where it is then transported via the AP3 pathway to the vacuolar membrane.[18] We speculate that Snx4-Atg20 and Snx4-Snx41 heterodimers coat distinct carriers.